Effects of Time-varying, Localized Heating on Tropical Circulations and Implications for Tropical Cyclogenesis

Jeffrey S. Gall and William M. Frank*
The Pennsylvania State University
University Park, Pennsylvania 16802

1. Introduction

This study investigates the behavior of the anomalous circulations of tropical waves, and in particular, how these waves enhance and modulate tropical cyclogenesis. Specifically, a numerical model was employed to examine and quantify the effects of tropical waves on the pre-genesis environmental vorticity, divergence, vertical shear, convection, and moisture. Results from this study will hopefully lead to a better understanding of the mechanisms by which tropical waves influence tropical cyclogenesis.

Numerous recent studies utilizing observational data for composite analyses have demonstrated that the anomalous circulations associated with various types of equatorially-trapped tropical waves provide an environment more favorable for tropical cyclogenesis (e.g. Maloney and Hartmann 2000; Molinari and Vollaro 2000; Hall et al. 2001; Bessafi and Wheeler 2006; Frank and Roundy 2006; Molinari et al. 2007). While much has been learned from these studies on how tropical waves influence tropical cyclogenesis, their methodology limits what can and cannot be learned concerning waves and tropical cyclogenesis. In these observational studies, it is tough to distinguish between cause and effect. Additionally, the magnitude of the anomaly associated with the various tropical waves may be obscured due to the averaging process of the composite analysis. For these reasons, a different approach was used to study the effects of tropical waves on tropical cyclogenesis.

*jsg229@psu.edu

2. Methodology

This study utilized a version of the Weather Research and Forecasting (WRF) model developed at the National Center for Atmospheric Research (NCAR) to be used as a Regional Climate Model (RCM; Leung et al. 2006). The model domain has a grid spacing of 36.025 km with 1112 x 255 grid points in the horizontal and 31 vertical levels. Such a configuration results in a domain that extends around the entire globe between 45° N and 30° S latitude. The model was initialized at 00Z on 17 May 1999. Periodic boundary conditions were used in the x-direction, while the north and south boundary conditions were generated with 1° GFS data. Monthly 1° SST data (AMIP data) was linearly interpolated in space to fit the 36 km grid. The SST data was also linearly interpolated in time such that the SST data were updated every 6 hours.

A six-species cloud microphysics package was used, which includes water vapor, rain water, cloud water, cloud ice, snow, and hail/graupel (Lin et al. 1983). The modified version of the Kain-Fritsch scheme (KF-Eta) was used to parametrize convective processes. This scheme is based on Kain and Fritsch (1990, 1993), but has been modified based on testing within the Eta model. As with the original KF scheme, it utilizes a simple cloud model with moist updrafts and downdrafts, including the effects of detrainment, entrainment, and relatively crude microphysics (Chen and Dudhia 2000). The atmospheric boundary layer is parametrized using the Yonsei University (YSU) scheme. This scheme is similar to the Medium Range Forecast (MRF) scheme (Hong and Pan 1996) in that it uses a so-called countergradient flux for heat and

moisture in unstable conditions, enhanced vertical flux coefficients in the boundary layer (BL), and handles vertical diffusion with an implicit local scheme. The scheme also explicitly treats entrainment processes at the top of the entrainment layer (Hong and Pan 1996; Hong et al. 2004; Noh et al. 2004). The Monin-Obukhov surface layer scheme is used to compute the surface exchange coefficients for heat, moisture, and momentum. The CAM radiation scheme was used to parametrize both longwave and shortwave radiation (Collins et al. 2004). Since this radiation scheme was designed to for implementation in general circulation climate models, it is well-suited for the model simulations.

Two simulations were performed using the WRF channel model - one control simulation (CON) and one simulation employing an idealized heat source. The structure of the heat source is based on the idealized heat source structure employed in Wheeler (2002) and is turned on and off over a 5 day period with a maximum heating of 10 K day $^{-1}$ at 2.5 days. The heat source is representative of the vertical heating profile of deep tropical convection (e.g. Song and Frank 1983; Frank and McBride 1989; Mapes 2000). Both the CON simulation and EXP2 simulation were run for 13 days and the heat source in EXP2 was turned on at t = 1 day.

3. Results

3a. *Control Simulation*

Fig. 1 and Fig. 2 shows the 13-day time-averaged 200 mb - 850 mb zonal shear and SST, respectively, for the latitude-longitude box bounded by 100° E - 120° W and 30° S - 45° N. The 200 mb - 850 mb zonal shear is westerly over a large portion of the domain section. An area of weak westerly to easterly zonal shear, however, is present over a large area of the West Pacific and the Maritime Continent. SSTs are a maximum near the equator and decrease rapidly poleward of 20° latitude. The warmest SSTs (303 K) are located in the West Pacific and a weak zonal SST gradient is also evident along the equator between the West and Central Pacific. Overall, the CON simulation produces a mean flow that strongly resembles major flow conditions observed in the tropics and sub-tropics. Furthermore, based on Fig. 1 and Fig. 2 (and other time-averaged quantities not shown), it is evident that the most favorable conditions for tropical cyclogenesis were located in the North West Pacific, i.e. in the longitude-latitude box bounded by approximately 120° E - 150° E and 0° - 20° N.

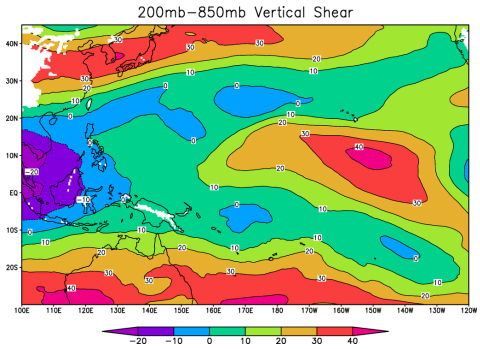

Figure 1: 13 day time-averaged 200 mb - 850 mb zonal wind shear.

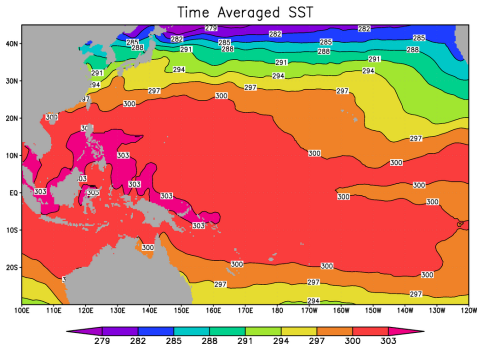

Figure 2: As in Fig. 1 except for SST (K).

The following criteria were used to classify a modeled disturbance as a tropical cyclone in the CON simulation:

1. maximum 10-m wind speed of at least 18 $m\ s^{-1}$ over the ocean equatorward of 25° latitude.
2. minimum sea level pressure of at least 1000 mb within 4° of the maximum wind speed location
3. Points one and two are valid over at least a continuous 24 hour period

While numerous tropical cyclones were identified throughout the CON simulation, no tropical cyclones formed within the region of interest (120° E - 150° E and 0° - 20° N) during the 13 day simulation.

3b. *EXP2 Simulation*

For this simulation, the heat source was centered at the dateline (180° E) and at the equator and was turned on at t = 1 day and off at t = 6 days. The initial conditions and N-S boundary conditions were the same as those employed for the CON simulation. Thus, the only difference between the two simulations was that the EXP2 run had a heat source. The criteria for classifying tropical cyclones in the CON simulation was also used for EXP2. In the EXP2 simulation one tropical cyclone (E1) formed within the region bounded by 120° E - 150° E and 0° - 20° N during the 13 day simulation and was first classified as such at t = 10 d. For analysis purposes, it was also necessary to classify the time at which the tropical cyclone first became a tropical depression using the following criteria:

1. A Maximum 10-m wind speed greater than 10 $m\ s^{-1}$
2. A sea level pressure deviation between the minimum central sea level pressure and the sea level pressure field 5° from the relative-minimum central pressure location of at least 1.5 mb in all four compass point directions.
3. Maximum 850 mb relative vorticity $\geq 1 \times 10^{-4} s^{-1}$ within 5° of local maximum wind 10-m wind speed

Using the tropical depression criteria listed above, E1 was first classified as a tropical depression at t = 8.5 d.

Fig. 3a-c shows the development of the tropical waves in response to the heat source at t = 3.25 d at 850 mb. The ellipse indicates the horizontal extent of the prescribed heat source, the triangle indicates the genesis location for the E1 storm, and the box indicates the region of interest where the large-scale conditions were most favorable for genesis. At this time, the flow at 850 mb at the E1 genesis location is nearly identical in both simulations (Fig. 3a and b). Closer to the heat source, however, large disparities are evident in the wind field. The EXP2 - CON 850 mb vector wind difference field clearly shows an eastward propagating Kelvin wave to the east of the heat source and the development of a westward propagating equatorial Rossby wave. Such a result is consistent with the analytic model of Gill (1980) for the response of the tropical atmosphere to prescribed large-scale heating.

Fig. 3d-f shows the flow at 850 mb at the time of E1 genesis (t = 8.5 d). A comparison of Fig. 3d to Fig. 3e reveals some major differences in the large-scale flow around the E1 genesis location at this time. In the CON simulation, the flow equatorward of the E1 genesis location is easterly from the dateline to 130° E and becomes westerly between 120° E and 130° E. The zonal flow in EXP2, however, is westerly between the equator and 8° N and 120° E - 160° E, and shifts to predominantly easterly flow north of 15° N over the same longitude band. The marked shift in zonal wind between the equator and 15° N within 120° E and 160° E is indicative of a monsoon trough, and it should be noted that the E1 genesis location resides near the center of the monsoon trough in a region of enhanced low-level vorticity. Although the wave structure is somewhat muted poleward of 5° (Fig. 3f) in the difference field, the westerly wind signal along the equator to the west of the heat source is indicative of a westward propagating equatorial Rossby wave and is most likely the reason for the enhancement of vorticity between 120° E and 160° E and 5° N - 15° N latitude.

Figure 4 shows the 200 mb-850 mb zonal and meridional wind shear averaged over a 4° box centered on the E1 genesis point for the EXP2 and CON simulations. Prior to t = -40 hr (time before E1 was classified as a depression), the zonal shear is nearly identical over the E1 genesis point. In comparing the EXP2-CON meridional shear to the EXP2-CON zonal shear, it is evident that a much larger difference exists in the magnitude of meridional shear than in the zonal shear. Furthermore, prior to E1 genesis, the meridional shear in the EXP2 simulation is less southerly than in the CON simulation. Based on the theoretical structure of an approaching equatorial Rossby wave and the latitude of the E1 genesis location, it would be expected that the wave would modulate the meridional shear much more than the zonal shear. Examination of Fig. 4 verifies this.

Figure 5 shows the 850 mb relative vorticity averaged over a 4° box centered on the E1 genesis point for the EXP2 and CON simulations. Prior to t = -60 hr, little dif-

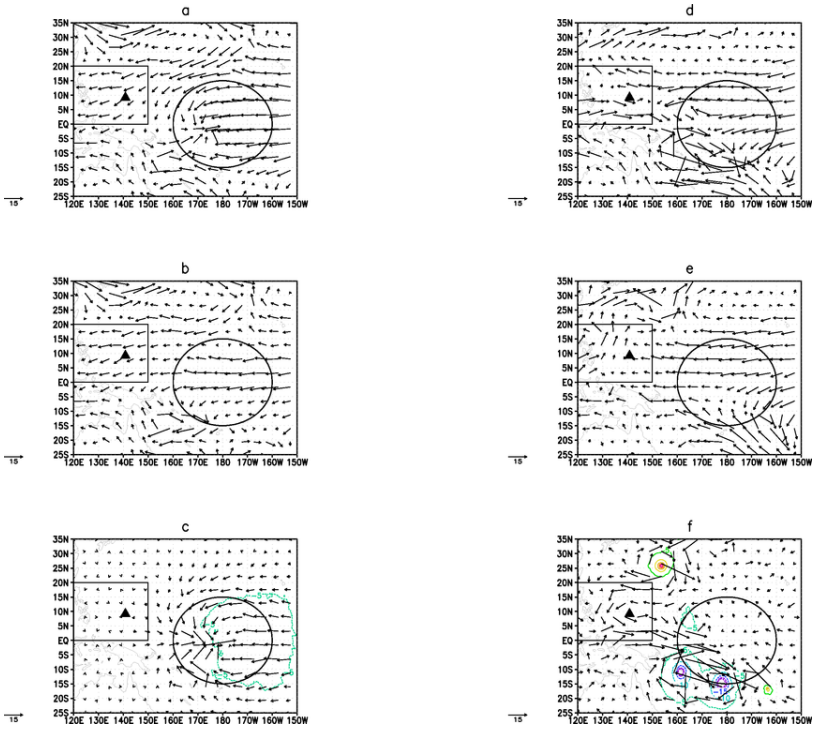

Figure 3: The 850 mb wind field for EXP2 (a), CON (b), and the EXP2-CON wind field and EXP2-CON sea level pressure (c; mb) at t = 3.25 d. The 850 mb wind field for EXP2 (d), CON (e), and the EXP2-CON wind field and EXP2-CON sea level pressure (f; mb) at t = 8.5 d. The ellipse indicates the horizontal extend of the heat source, the triangle indicates the E1 genesis location, and the rectangular box identifies the location of favorable large-scale conditions for genesis.

ference exists between the CON and EXP2 simulations. From t = -60 hr to t = 0 (time of genesis), the relative vorticity in the EXP2 simulation increases rapidly until reaching a value of 6×10^{-5} s^{-1} at t = 0. Conversely, the CON relative vorticity decreases over this same period such that by t = 0, the box-averaged relative vorticity is -1×10^{-5} s^{-1}, indicative of weak anticyclonic vorticity.

Figure 5 also shows the 925 mb divergence averaged over a 4° box centered on the E1 genesis point. Prior to t = -66 hr, there is little difference between the EXP2 and CON 925 mb divergence field. From t = -60 hr to t = 24 hr, the EXP2 box-averaged divergence becomes increasingly convergent such that by t = 12 hr a maximum value of approximately -2.5×10^{-5}s^{-1} is achieved. Over the same time period, however, the CON simulation switches from weakly convergent to weakly divergent.

4. Discussion

From inspection of Figs. 4 and 5, it is clearly evident that the dynamical environment of the E1 genesis location became more favorable for tropical cyclogenesis as indicated by the large increase in low-level cyclonic relative vorticity, low-level convergence, and decrease in vertical shear. It appears that the modulation of the dynamical fields via the propagating equatorial Rossby wave plays a crucial role in the development of the E1 tropical cyclone.

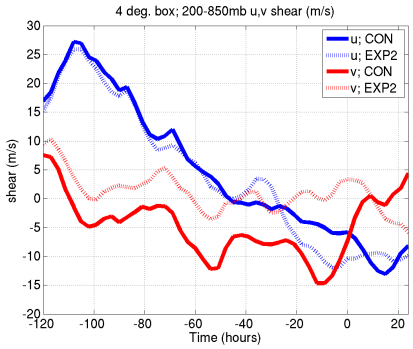

Figure 4: Time series of the 200 mb-850 mb zonal and meridional wind shear averaged over a 4° box centered on the E1 genesis point for EXP2 and CON. Time is plotted relative to genesis time, whereby negative times indicate hours before genesis.

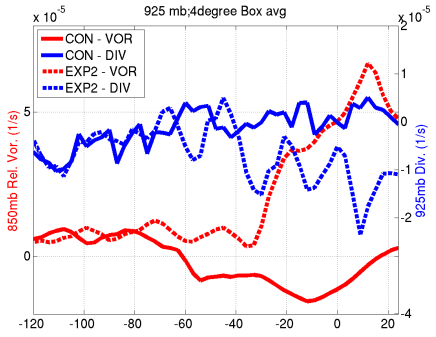

Figure 5: As in Fig. 4 except for EXP2 and CON 850 mb relative vorticity and 925 mb divergence.

At the time of this writing, only two simulations have been conducted - one control (CON) simulation and one simulation with the artificial heat source turned on (EXP2). While it is tough to draw concrete conclusions based on one experimental simulation, these results warrant the need for additional simulations. The important aspect of this methodology is that the magnitude of the anomalous circulations associated with the various generated tropical waves can be controlled to an extent via the heat source specifications. As a result of the varying wave structures and intensities, tropical cyclogenesis may occur in certain simulations but not others in regions influenced by the propagating waves. Such a result may be significant in that it will allow for quantification of the anomalous circulations of the tropical wave at the time and place of genesis and provide a better understanding of the mechanisms by which tropical waves influence tropical cyclogenesis.

References

Bessafi, M. and M. Wheeler, 2006: Modulation of south indian ocean tropical cyclones by the madden-julian oscillation and convectively coupled equatorial waves. *Mon. Wea. Rev.*, **134**, 638–656.

Chen, F. and J. Dudhia, 2000: *Annual report*. WRF Physics.

Collins, W., P. J. Rasch, and Others, 2004: Description of the ncar community atmosphere model (cam 3.0). Technical report, National Center for Atmospheric Research, Boulder, CO.

Frank, W. M. and J. L. McBride, 1989: The vertical distribution of heating in amex and gate cloud clusters. *J. Atmos. Sci.*, **46**, 3464–3478.

Frank, W. M. and P. E. Roundy, 2006: The role of tropical waves in tropical cyclogenesis. *Mon. Wea. Rev.*, **134**, 2397–2417.

Gill, A. E., 1980: Some simple solutions for heat-induced tropical circulation. *Quart. J. Roy. Meteor. Soc*, **106**, 447–462.

Hall, J. D., A. J. Matthews, and D. J. Karoly, 2001: The modulation of tropical cyclone activity in the australian region by the madden-julian oscillation. *Mon. Wea. Rev.*, **129**, 2970–2982.

Hong, S. Y., J. Dudhia, and S. H. Chen, 2004: A revised approach to ice microphysical processes for the bulk parameterization of clouds and precipitation. *Mon. Wea. Rev.*, **132**, 103–120.

Hong, S. Y. and H. L. Pan, 1996: Nonlocal boundary layer vertical diffusion in a medium-range forecast model. *Mon. Wea. Rev.*, **124**, 2322–2339.

Kain, J. S. and J. M. Fritsch, 1990: A one-dimensional entraining/detraining plume model and its application in convective parameterization. *J. Atmos. Sci.*, 2784–2802.

— 1993: Convective parameterization for mesoscale models: The kain-fritsch scheme. *The Representation of Cumulus Convection in Numerical Models, Meteor. Monogr.*, amer. Meteor. Soc., 165-170.

Leung, L. R., B. Kuo, J. Tribbia, G. Holland, J. Dudhia, J. Done, B. Collins, J. Hack, B. Large, J. Hurrell, R. Anthes, M. Moncrieff, J. Michalakes, T. Henderson, J. Caron, C. Bruyere, and W. Wang, 2006: Analysis and evaluation of wrf tropical channel simulations. *7th WRF Users' Workshop*.

Lin, Y. L., R. D. Farley, and H. D. Orville, 1983: ulk parameterization of the snow field in a cloud model. *J. Appl. Meteor.*, **22**, 1065–1092.

Maloney, E. and D. Hartmann, 2000: Modulation of eastern north pacific hurricanes by the madden-julian oscillation. *J. Climate*, **13**, 1451–1460.

Mapes, B. E., 2000: Convective inhibition, subgrid-scale triggering energy, and stratiform instability in a toy tropical wave model. *J. Atmos. Sci.*, **57**, 1515–1535.

Molinari, J., K. Lombardo, and D. Vollaro, 2007: Tropical cyclogenesis within an equatorial rossby wave packet. *J. Atmos. Sci.*, **64**, 1301–1317.

Molinari, J. and D. Vollaro, 2000: Planetary- and synoptic-scale influences on eastern pacific tropical cyclogenesis. *Mon. Wea. Rev.*, **128**, 3296–3307.

Noh, Y., W. G. Chun, S. Y. Hong, and S. Raasch, 2004: Improvement of the k-profile model for the planetary boundary layer based on large eddy simulation data. *Boundary Layer Meteorology*, **107**, 401–427.

Song, J. L. and W. M. Frank, 1983: Relationships between deep convection and large-scale processes during gate. *Mon. Wea. Rev.*, **111**, 2145–2160.

Wheeler, M., 2002: *Tropical Meteorology: Equatorial Waves*, volume 1. Academic Press, 2313-2325 pp.